ACS OMEGA

http://pubs.acs.org/journal/acsodf

Article

Magnetic Molecularly Imprinted Polymer for the Selective Enrichment of Glyphosate, Glufosinate, and Aminomethylphosphonic Acid Prior to High-Performance Liquid Chromatography

Nilawan Surapong and Rodjana Burakham*

Cite This: *ACS Omega* 2021, 6, 27007−27016

Read Online

ACCESS | Metrics & More | Article Recommendations | Supporting Information

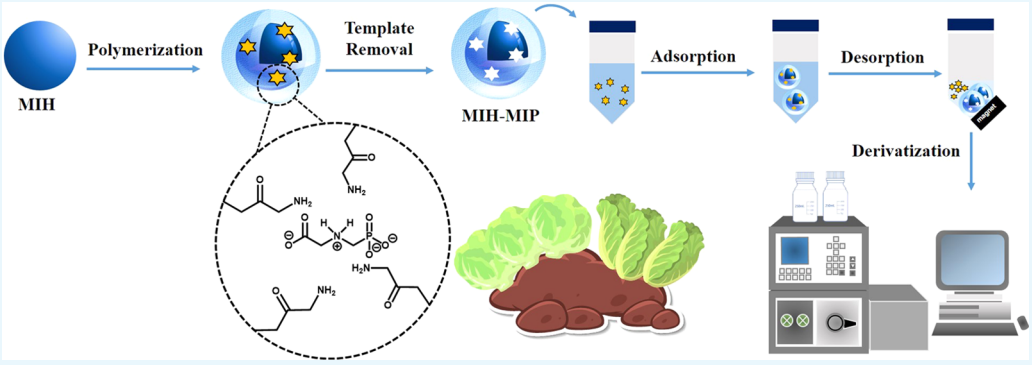

ABSTRACT: A novel mixed iron hydroxide molecularly imprinted polymer (MIH-MIP) was synthesized via polymerization using mixed-valence iron hydroxide as a magnetic supporter, glyphosate as a template, acrylamide as a functional monomer, and ethylene glycol dimethacrylate as a cross-linker. The resulting material was characterized and applied as a sorbent for the selective enrichment of glyphosate, aminomethylphosphonic acid, and glufosinate by magnetic solid-phase extraction (MSPE) prior to high-performance liquid chromatography. MIH-MIP possessed a high adsorption capacity in the range of 2.31−5.40 mg g^{-1} with good imprinting factors ranging from 1.52 to 7.59. The Langmuir model proved that the recognition sites were distributed as a monolayer on the surface of MIH-MIP. Scatchard analysis showed two types of binding sites on MIH-MIP. The kinetic characteristics of MIH-MIP suggested that the binding process of all analytes fit well with the pseudosecond-order model. The developed methodology provides good linearity in the range of 72.0−2000.0 $\mu g\ L^{-1}$. Low detection limits of 21.0−22.5 $\mu g\ L^{-1}$ and enrichment factors of up to 18 were achieved. The precision in terms of relative standard deviations of the intra- and interday experiments was better than 7 and 9%, respectively. The applicability of the developed MSPE facilitates the accurate and efficient determination of water, soil, and vegetable samples with satisfactory recoveries in the range of 86−118%. The results confirmed the suitability of the MIH-MIP sorbent for selective extraction and quantification of glyphosate, aminomethylphosphonic acid, and glufosinate.

1. INTRODUCTION

Glyphosate (*N*-(phosphonomethyl)glycine, GLYP) and glufosinate (2-amino-4-(hydroxymethylphosphinyl)butyric acid, GLUP) are the most frequently used nonselective herbicides for weed control in agricultural production. GLYP is nonpersistent in the environment and is rapidly degraded due to light and microorganisms, resulting in aminomethylphosphonic acid (AMPA) as a major metabolite. These compounds are challenging to analyze due to their small size structures, high polarity, and lack of a chromophore or fluorophore. Separation techniques, including gas chromatography (GC), high-performance liquid chromatography (HPLC), and capillary electrophoresis (CE), are commonly used for the determination of GLYP and related compounds.[1,2] The physicochemical characteristics and a high sample matrix make the detection of these compounds at trace levels difficult. Hence, a sample preparation or preconcentration step is required before instrumental analysis.

Solid-phase extraction (SPE) is a popular and practical sample preparation technique due to its high recovery, high enrichment factor, wide applicable range for organic analytes (from nonpolar to very polar analytes), and ease of

Received: July 2, 2021
Accepted: September 30, 2021
Published: October 8, 2021

https://doi.org/10.1021/acsomega.1c03488
ACS Omega 2021, 6, 27007−27016

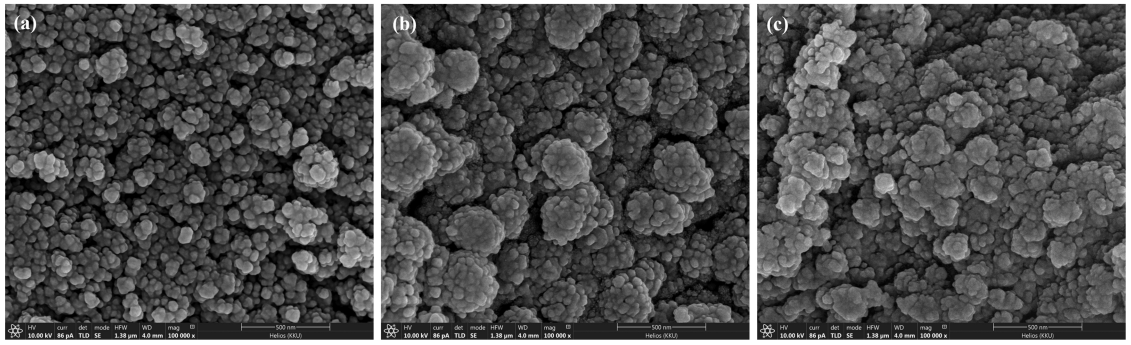

Figure 1. SEM micrographs of (a) MIH, (b) MIH-MIP, and (c) MIH-NIP.

automation, while liquid−liquid extraction (LLE) has some drawbacks, such as being time-consuming, requiring a larger amount of solvent, and being laborious. Recently, analytical chemists have turned to SPE-based miniaturized and simplified techniques. Dispersive solid-phase extraction (DSPE) is proposed. Such a method is based on the dispersion of micro- or nanosorbents (in the μg or mg range) in the sample solution to contribute to the interaction between solid sorbent and analytes and isolation of solid sorbent by centrifugation and filtration. After adsorption, the analytes adsorbed in the solid sorbent are eluted. Magnetic solid-phase extraction (MSPE) is one of the most effective SPE operating techniques based on dispersive mode. Magnetic materials have been employed for the extraction of the target analytes and then simply separated by the application of an external magnetic field. The essential features of the MSPE technique are that it is simple and has rapid solid-phase separation, diminished extraction time, and less organic solvent consumption than conventional SPE.

The enrichment sorbents of GLYP are based on either ion exchange or partitioning of its derivatives on nonpolar sorbents.[3] However, the methods are poorly selective toward GLYP in the presence of compounds of a similar chemical nature, thus causing interference in the derivatization and detection steps. Molecularly imprinted polymers (MIPs) have received great attention in recent decades in many scientific areas, such as chemical sensors,[4−7] chromatographic stationary phases,[8,9] and SPE sorbents.[10−13] In the field of sample preparation technology, MIP materials are specific or highly selective sorbents. Different synthesis protocols have been adopted for preparing MIPs for GLYP.[10−12]

Magnetic molecularly imprinted polymers (MMIPs) have the benefits of highly selective recognition cavities with outstanding magnetism, which can be easily separated from the solution using an external magnet without tedious centrifugation or filtration.[14] The combination of magnetic materials and molecular imprinting technology can compensate for the shortcomings of traditional MIPs for application in sorbent-based extraction procedures. MMIPs have been applied for the determination of pesticides, i.e., carbamate,[15] pyrethroids,[16,17] triazine,[18] organophosphorus,[19−21] and imidacloprid.[22] To the best of our knowledge, only one MMIP for GLYP has been synthesized, based on Fe_3O_4 as the magnetic core and polymethylmethacrylate as the shell, using ammonium persulfate as an initiator for free radical polymerization and glutaraldehyde as a cross-linker.[23] The synthesized nanocomposite was used to modify the glassy carbon electrode to investigate the recognition of GLYP. However, there is a lack of literature dedicated to the development of MMIP for the enrichment of GLYP and its analogues. Thus, it is important to further develop MMIP for use as an adsorbent in the MSPE technique.

In the present work, we propose a novel synthesized MMIP using mixed-valence iron hydroxide as a magnetic supporter, GLYP as a template, acrylamide (AAm) as a functional monomer, and ethylene glycol dimethacrylate (EGDMA) as a cross-linker. The proposed material is called a mixed iron hydroxide molecularly imprinted polymer (MIH-MIP). We also developed, for the first time, the MSPE procedure using MMIP as a selective sorbent for the enrichment of GLYP and its analogues. The extract was derivatized with 9-fluorenylmethoxycarbonyl chloride (FMOC-Cl) before analysis by HPLC. The characteristics, binding experiments, and selectivity of MIH-MIP were also investigated. The proposed material showed satisfactory magnetization properties, specific recognition ability, and fast adsorption kinetics toward the target analytes. The developed MSPE coupled with the HPLC procedure has been successfully applied to determine GLYP, AMPA, and GLUP in various environmental samples.

2. RESULTS AND DISCUSSION

2.1. Characterization. The functional groups of the synthesized sorbents were determined using Fourier transform infrared spectroscopy (FTIR), as shown in Figure S1. The FTIR spectra of the synthesized polymers agree well with those of polyacrylamide.[10] The aliphatic C−H stretching vibration peaks of methyl and methylene were found at 2996 and 2953 cm^{-1}, respectively. The peaks at 1726 and 1645 cm^{-1} were attributed to the stretching of carbonyl (C═O) from EGDMA and AAm, respectively. The 1450 cm^{-1} band was assigned to the angular deformity of CH_2 (scissors), presented in the EGDMA structure. At 1255 cm^{-1}, the stretching of C−N in AAm was observed. The 1157 cm^{-1} band was related to the C−O stretching of the ester group in EGDMA. The peak at 636 cm^{-1} originating from Fe−O vibration was found in the spectra of both polymer composites. The results indicated that EGDMA and monomers successfully formed polymers with the magnetic material (MIH). In addition, similar characteristic signals were observed for MIH-NIP. The results confirmed the complete removal of the template molecules from MIH-MIP.

The X-ray diffraction (XRD) patterns of the as-synthesized MIH, MIH-MIP, and MIH-NIP are shown in Figure S2. The characteristic peaks of the MIH material agree with a previous report.[24] The diffraction peaks with 2θ values of 30.2, 35.6, 43.3, 53.7, 57.3, and 62.9° correspond to the (220), (311),

https://doi.org/10.1021/acsomega.1c03488
ACS Omega 2021, 6, 27007−27016

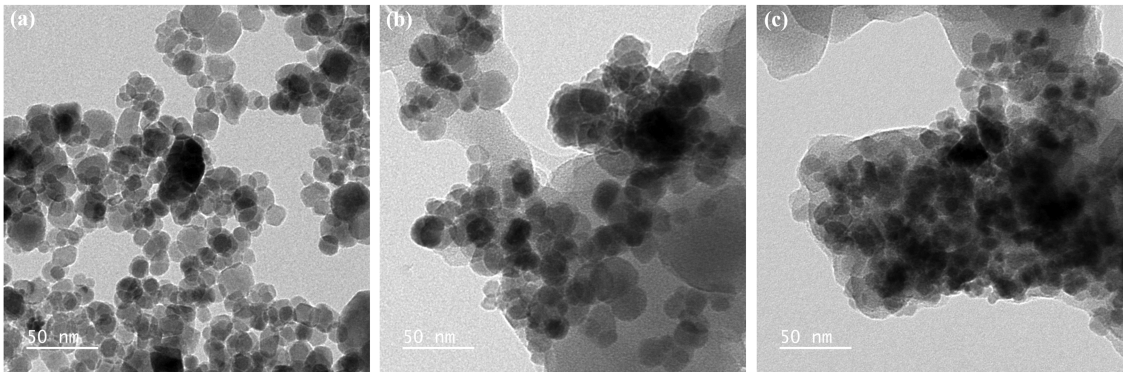

Figure 2. TEM images of (a) MIH, (b) MIH-MIP, and (c) MIH-NIP.

(400), (422), (511), and (440) crystal planes of the crystalline Fe_3O_4/γ-Fe_2O_3 phase; these agree with the standard data JCPDS card nos. 39-1346 and 75-0033 for γ-Fe_2O_3 and Fe_3O_4, respectively. The XRD patterns of the synthesized MIH-MIP and MIH-NIP were not different, and the crystal structure of the magnetic material remained the same after polymerization. A decrease in the diffraction peaks of the magnetic polymer sorbents could be due to obstruction of the MIH crystal phase by the amorphous polymer material.

The morphology of MIH, MIH-MIP, and MIH-NIP was investigated by scanning electron microscopy (SEM), as shown in Figure 1. The SEM image of the synthesized MIH shows agglomerated nanoparticles (Figure 1a). The surface morphology of MIH-MIP and MIH-NIP shown in Figure 1b,c, respectively, was different from that of MIH nanoparticles because of the polyacrylamide coating, which offered evidence of the formation of a polymer. Figure 2 shows transmission electron microscopy (TEM) micrographs of the synthesized materials. Covering of the polyacrylamide shell over MIH nanoparticles was clearly observed from the TEM images of MIH-MIP and MIH-NIP.

An elemental CHN analysis was carried out to confirm the carbon, hydrogen, and nitrogen compositions of MIH-MIP and MIH-NIP. The results indicated that the two magnetic polymers had similar compositions. The percentages of C/H/N in MIH-MIP and MIH-NIP were 46.16:5.97:0.51 and 43.63:5.72:0.37, respectively. These results also confirmed the successful removal of the template molecules from MIH-MIP.

The magnetic properties of the sorbents were measured using a vibrating sample magnetometer (VSM), as shown in Figure 3. The saturation magnetization values of MIH, MIP-MIH, and MIH-NIP were 98.627, 18.931, and 20.954 emu g^{-1}, respectively. The decrease in magnetization values could be attributed to the coating of the polymeric layer on the magnetic material. Although their magnetization was significantly reduced, the magnetic strengths (above 10 emu g^{-1}) of these materials were sufficient for application in the MSPE method. The inset of Figure 3 shows a clear solution after applying an external magnet for 20 s on the gray MIH-MIP suspension.

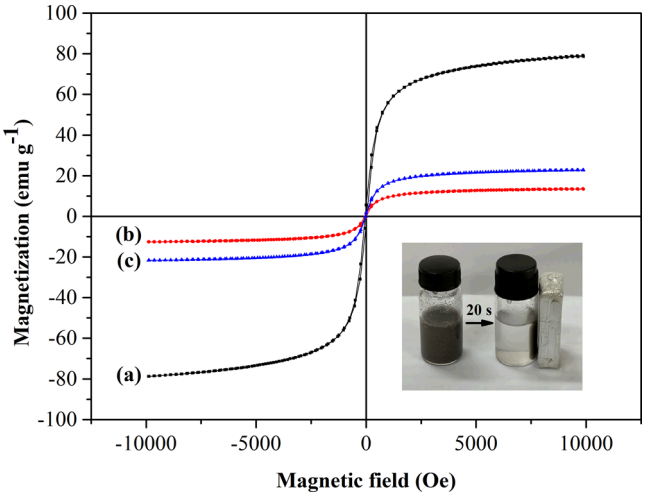

Figure 3. VSM plots of (a) MIH, (b) MIH-MIP, and (c) MIH-NIP (the inset shows the separation of MIH-MIP by an external magnet).

2.2. Binding Studies. *2.2.1. Adsorption Isotherms.* The adsorption isotherms of MIH-MIP and MIH-NIP are shown in Figure S3. The adsorption amounts of the target analytes on MIH-MIP and MIH-NIP increased with increasing initial concentrations until reaching saturation levels. MIH-MIP showed adsorption capacities of 5.40, 2.31, and 2.42 mg g^{-1} for GHYP, AMPA, and GLUP, respectively. The higher adsorption ability of MIH-MIP than that of MIH-NIP indicated that it possessed abundant imprinted cavities, leading to higher selective recognition for GLYP, AMPA, and GLUP.

Scatchard analysis was used to investigate the binding characteristics of MIH-MIP toward GLYP, AMPA, and GLUP. As shown in Figure 4, Scatchard's plot of MIH-MIP for each studied compound consisted of two linear parts (red and black lines), which suggested the presence of two types of binding sites on the MIH-MIP surface. This result corresponded with the characteristics of the previously reported molecular imprinting sensor of GLYP.[25] The linear equations as well as K_d and Q_{max} values calculated from the slopes and intercepts are summarized in Table S1. In contrast, MIH-NIP showed only one straight line (b1). Considering the K_d values, MIH-MIP contains low- and high-affinity binding sites for specifically adsorbing GLYP, AMPA, and GLUP, while MIH-NIP had only one negligible affinity binding site for adsorbing GLYP, AMPA, and GLUP nonspecifically. These results confirmed that the as-prepared MIH-MIP showed good binding ability for all studied analytes.

The Langmuir and Freundlich isotherms for GLYP, AMPA, and GLUP are shown in Figure S4. The results demonstrated that the Langmuir model was more suitable than the Freundlich model. Therefore, the recognition sites were uniformly distributed in a monolayer on the surface of MIH-MIP and MIH-NIP.

https://doi.org/10.1021/acsomega.1c03488
ACS Omega 2021, 6, 27007−27016

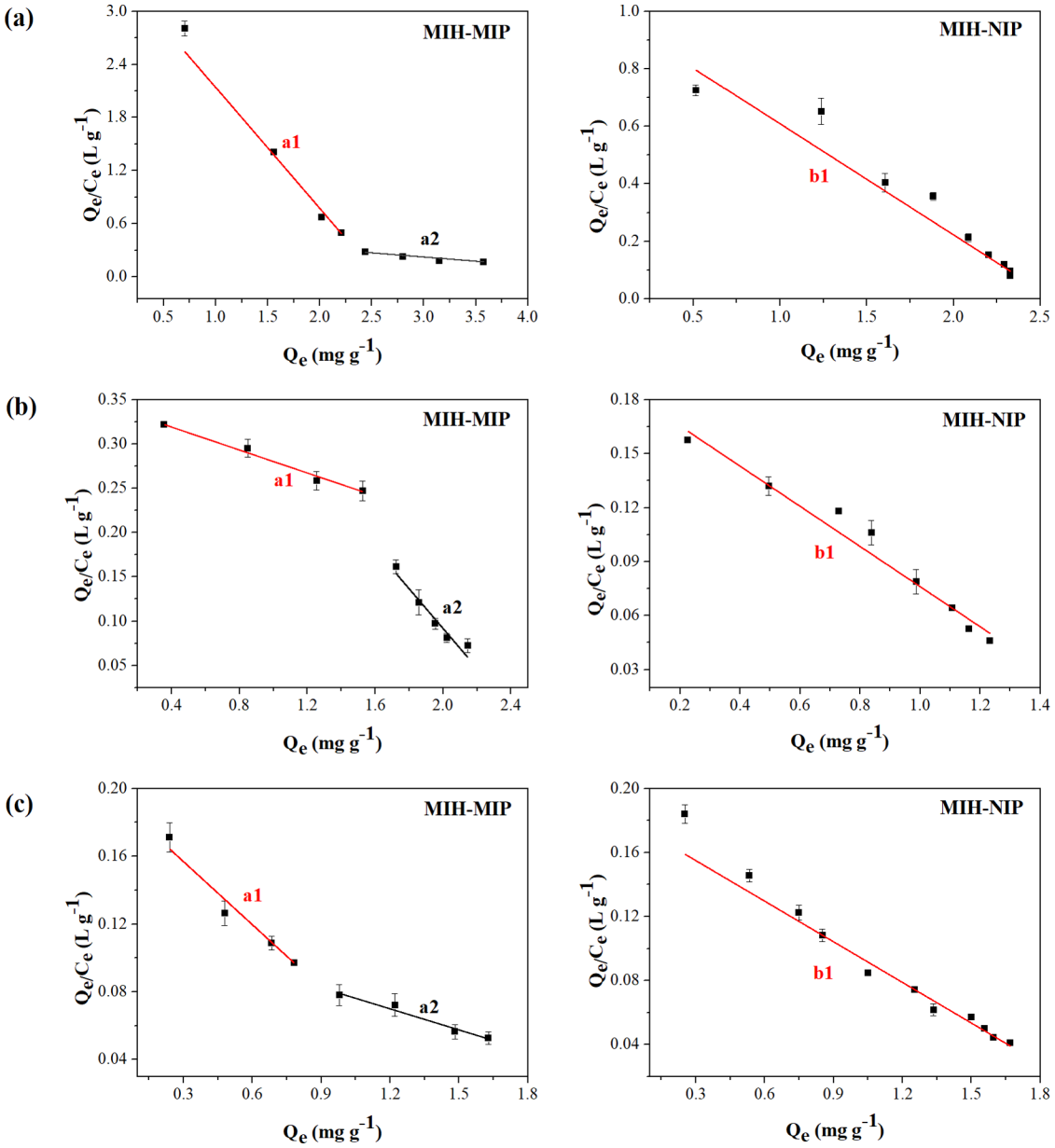

Figure 4. Scatchard plots of MIH-MIP and MIH-NIP for (a) GLYP, (b) AMPA, and (c) GLUP.

2.2.2. Adsorption Kinetics. The dynamic adsorption of GLYP, AMPA, and GLUP onto MIH-MIP and MIH-NIP is illustrated in Figure S5. It was observed that the adsorbed amounts of analytes (Q) by the two magnetic polymers increased with time. During the first 60 s, the adsorption amounts on MIH-MIP increased rapidly and gradually reached equilibrium after 80 s. MIH-NIP also showed a similar trend as MIH-MIP but with lower adsorbed amounts than MIH-MIP for all studied compounds (Figure S5a,d,g). Moreover, the equilibrium adsorption ability of MIH-MIP for GLYP was higher than that of other analytes, which was in accordance with static adsorption results.

Data obtained from kinetic models, including pseudofirst-order (Figure S5b,e,h) and pseudosecond-order (Figure S5c,f,i), are summarized in Table S2. The pseudosecond-order equations provided better R_2 values than the pseudofirst-order equations. Therefore, the pseudosecond-order model was the best fit for MIH-MIP and MIH-NIP. In addition, the equilibrium adsorption capacity (Q_e) from the experiment was closer to Q_{2cal} than Q_{1cal}. This result was in accordance with a previous report.[10] The pseudosecond-order model proposes that the target compounds (GLYP, AMPA, and GLUP) bind to two or more active sites on the adsorbent surface, and this adsorption is of a chemical nature.[26]

2.3. Selectivity of MIH-MIP. In the present study, AMPA, GLUP, and glycine (GLYC) were selected as analogues, and sarcosine (SAR) and monocrotophos (MONO) were selected as nonanalogues to investigate the selectivity of MIH-MIP toward GLYP. The results are shown in Figure 5. The highest imprinting factor (IF) value of GLYP on MIH-MIP (7.59) suggested that MIH-MIP had the highest affinity for GLYP (the template molecule) compared to the other compounds. The IF values of MIH-MIP for GLYP analogues were better than those of nonanalogues, which agreed well with the selectivity coefficient (SC) values (1.86 for AMPA, 4.98 for GLUP, 2.21 for GLYC, 8.09 for SARC, and 7.55 for MONO).

https://doi.org/10.1021/acsomega.1c03488
ACS Omega 2021, 6, 27007−27016

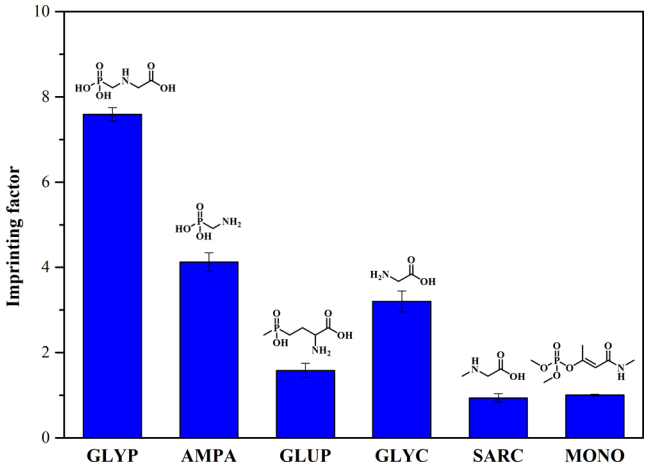

Figure 5. Selectivity of MIH-MIP (condition: 20 mg of MIH-MIP or MIH-NIP sorbent, 10 mL of mixed solutions of GLYP, AMPA, GLUP, GLY, SAR, and MONO at a concentration of 20 μg mL^{-1} each, and 80 s of vortexing).

These results are probably related to the similarity of functional groups, which can generate hydrogen bonds, as in GLYP.[27] In the present work, both electrostatic interactions and hydrogen bonds can also occur between the interference and the functional monomer. However, the template molecule has a high adsorbed amount because the interaction between the polymer imprinted and the target analyte was not only dependent on electrostatic interactions and hydrogen bonding but also related to the specific cavity memory of the size, shape, and functional group of the template.[28] Therefore, MIH-MIP demonstrated specific recognition sites for the class-selective extraction of GLYP analogues.

2.4. Optimization of the MSPE Condition. To obtain satisfactory MSPE conditions for the target analytes, the experimental parameters influencing the extraction efficiency were investigated, including sample volume, sorbent amount, adsorption and desorption times, type of desorption solvent and its volume, and sample pH. A mixed standard solution containing 0.5 mg L^{-1} GLYP, AMPA, and GLUP was used to examine the extraction performance of the MSPE method under different experimental conditions. All optimization experiments were carried out in triplicate (n = 3). Peak areas were used to evaluate the extraction efficiency of the developed procedure.

The effect of sample volume on the extraction efficiency of the target analytes was assessed in the range from 10 to 35 mL while keeping other conditions as follows: 50 mg of sorbent, a vortex adsorption time of 60 s, 1000 μL of 0.01 mol L^{-1} NaOH as desorption solvent, and a vortex desorption time of 60 s. The results in Figure S6 show that the peak areas of all analytes increased as the sample volume increased from 10 to 25 mL and remained constant afterward. Therefore, a sample volume of 25 mL was selected for subsequent experiments.

To achieve the highest extraction efficiency, different amounts of MIH-MIP ranging from 50 to 150 mg were examined to extract the studied herbicides. The other experimental conditions were fixed as follows: 25 mL of the sample solution, a vortex adsorption time of 60 s, 1000 μL of 0.01 mol L^{-1} NaOH as desorption solvent, and a vortex desorption time of 60 s. The peak areas of all analytes reached a plateau using the sorbent in the range from 100 to 150 mg (Figure S7). Therefore, in the present work, a sorbent amount of 100 mg was chosen.

The time during the extraction process generally determines the equilibrium distribution of the analytes between the aqueous sample solution and the sorbent material. In the present work, vortex agitation was applied during extraction to accelerate the adsorption kinetics of the target herbicides onto the MIH-MIP sorbent. The vortex adsorption time varied in the range of 20−100 s. The other experimental conditions were fixed as follows: 100 mg of sorbent, 25 mL of the sample solution, 1000 μL of 0.01 mol L^{-1} NaOH as the desorption solvent, and a vortex desorption time of 60 s. The extraction efficiency in terms of peak area increased with increasing vortex time from 20 to 80 s and remained constant after this point, as shown in Figure S8a. Therefore, vortexing was applied during the adsorption process for 80 s before collecting the MIH-MIP sorbent from the sample solution.

During the desorption process, the analytes retaining MIH-MIP sorbents were suspended in the desorption solvent using a vortex mixer, and a sufficient desorption time was required to quantitatively desorb the analytes from the sorbent. Therefore, the vortex desorption time between 20 and 100 s was investigated while keeping the other parameters as follows: 100 mg of sorbent, 25 mL of the sample solution, a vortex adsorption time of 80 s, and 1000 μL of 0.01 mol L^{-1} NaOH as desorption solvent. The results in Figure S8b indicated that the peak areas of all analytes reached the maximum at 60 s. Hence, a vortex time of 60 s was sufficient for achieving the complete desorption of analytes from the MIH-MIP sorbent and therefore was selected in this work.

Desorption of analytes from the solid sorbent is an important part of the entire extraction process. To obtain high desorption efficiency, different types of desorption solvents were tested, including 0.01 mol L^{-1} NaOH, 0.01 mol L^{-1} NH_4OH, acetonitrile: 0.1 mol L^{-1} NaOH (90:10% v/v), acetone: 0.1 mol L^{-1} NaOH (90:10% v/v), and methanol: 0.1 mol L^{-1} NaOH (90:10% v/v). The other experimental conditions were fixed as follows: 100 mg of sorbent, 25 mL of the sample solution, a vortex adsorption time of 80 s, 1000 μL desorption solvent volume, and a vortex desorption time of 60 s. As shown in Figure S9a, a 0.01 mol L^{-1} NaOH solution gave the highest desorption power for all studied analytes and was adopted throughout the work.

To study the effect of desorption solvent volume on the extraction efficiency of MSPE, the volume of 0.01 mol L^{-1} NaOH varied in the range of 400−800 μL. The other experimental conditions were fixed as follows: 100 mg of sorbent, 25 mL of the sample solution, a vortex adsorption time of 80 s, and a vortex desorption time of 60 s. The results in Figure S9b show that sufficient elution efficiency was achieved when 500 μL of 0.01 mol L^{-1} NaOH was used. Therefore, after extraction, the analytes were desorbed using 500 μL of 0.01 mol L^{-1} NaOH before further derivatization with the FMOC-Cl reagent.

GLYP and AMPA are amphiprotic compounds, with pK_a values of 0.8, 2.3, 6.0, and 11.0 for GLY and 0.9, 5.6, and 10.2 for AMPA.[29] Depending on the pH of the sample solution, GLYP and AMPA can be either positively or negatively charged. The influence of sample pH values ranging between 4 and 11 was investigated while keeping other experimental parameters at constant: 100 mg of sorbent, 25 mL of the sample solution, a vortex adsorption time of 80 s, 500 μL of 0.01 mol L^{-1} NaOH as desorption solvent, and a vortex

https://doi.org/10.1021/acsomega.1c03488
ACS Omega 2021, 6, 27007−27016

Table 1. Analytical Features of Direct HPLC and the Proposed MSPE-HPLC Procedures

analyte	method	LOD (μg L^{-1})	LOQ (μg L^{-1})	precision (%RSD) intraday (n = 7)	precision (%RSD) interday (n = 5 × 3)	linear range (μg L^{-1})	linear equation	R^2	EF
GLYP	direct HPLC	750.0	2500.0	3	6	2500.0−15 000.0	y = 7.8903x + 4137.6	0.9991	18
	MSPE-HPLC	21.0	72.0	5	8	72.0−2000.0	y = 140.82x + 1433.8	0.9912	
AMPA	direct HPLC	450.0	1500.0	6	8	1500.0−15 000.0	y = 24.997x − 25 689	0.9965	14
	MSPE-HPLC	22.0	73.5	3	4	73.5−2000.0	y = 348.22x − 14 077	0.9902	
GLUP	direct HPLC	450.0	1500.0	2	4	1500.0−15 000.0	y = 15.335x + 3902.8	0.9980	9
	MSPE-HPLC	22.5	75.0	7	9	75.0−2000.0	y = 137.38x + 15 650	0.9982	

Table 2. Recoveries for Determination of Real Samples Using the Proposed MSPE-HPLC Procedure

sample	GLYP[a] found (mg kg^{-1})	GLYP %R_1 (%RSD)	GLYP %R_2 (%RSD)	AMPA[b] found (mg kg^{-1})	AMPA %R_1 (%RSD)	AMPA %R_2 (%RSD)	GLUP found (mg kg^{-1})	GLUP %R_1 (%RSD)	GLUP %R_2 (%RSD)
tap water	ND	88 (3)	104 (2)	ND	86 (7)	98 (3)	ND	88 (2)	103 (2)
rice field water	ND	112 (9)	92 (5)	ND	107 (2)	97 (6)	ND	106 (6)	96 (2)
agricultural water	ND	107 (8)	115 (3)	ND	97 (4)	105 (1)	ND	90 (9)	89 (2)
river water	ND	98 (4)	108 (9)	ND	112 (4)	98 (5)	ND	95 (3)	92 (3)
rice field soil	ND	92 (6)	109 (3)	ND	94 (10)	103 (2)	ND	97 (3)	91 (7)
agricultural soil	ND	94 (8)	99 (3)	ND	110 (1)	90 (3)	ND	112 (6)	94 (6)
Chinese cabbage	0.85	118 (6)	95 (6)	0.87	104 (2)	87 (5)	ND	86 (8)	89 (6)
cabbage	ND	98 (3)	103 (2)	ND	106 (3)	91 (9)	ND	91 (9)	96 (4)

[a]Spiked concentration: R_1 = LOQ and R_2 = 5LOQ. [b]ND, not detected.

desorption time of 60 s. According to the results in Figure S10, the extraction efficiency of all analytes increased by increasing the sample pH from 4 to 7. This could be due to the increase in the number of negative charges of the analytes from ionization of phosphonate and carboxylate groups. Conversely, acrylamide is positively charged.[10] At higher pH values (9−10), all functional groups are deprotonated, and the negative charge is maximal, leading to a dramatic drop in extraction efficiency. Therefore, in the present work, the sample pH was controlled at 7 during extraction. Under the selected MSPE conditions, specifically, 25 mL of the sample solution, 100 mg of MIH-MIP as a sorbent, a vortex adsorption time of 80 s, a vortex desorption time of 60 s, 500 μL of 0.01 mol L^{-1} NaOH as desorption solvent, and a sample pH of 7, the extraction recoveries of GLYP, AMPA, and GLUP were 96.1, 72.5, and 23.4%, respectively. The developed MSPE method using MIH-MIP provided high extraction efficiency for GLYP (template molecule). The results also corresponded to the selectivity data.

2.5. Method Validation. The analytical performance of the developed MSPE-HPLC method for the determination of GLYP, AMPA, and GLUP was evaluated under the above-mentioned conditions. Linear calibration graphs were obtained in the ranges of 72.0−2000.0, 73.5−2000, and 75.0−2000.0 μg L^{-1} for GLYP, AMPA, and GLUP, respectively, with coefficients of determination (R_2) greater than 0.9902. The limits of detection (LODs) and limits of quantification (LOQs) were calculated from the concentrations giving signal-to-noise ratios of 3 and 10, respectively, and were obtained in the ranges of 21.0−22.5 and 72.0−75.0 μg L^{-1}, respectively. The LOQs obtained by the proposed method are lower than the maximum residue limits (MRLs) of glyphosate (0.1 mg kg^{-1} in raw agricultural commodities) established by the European Commission (EC No. 396/2005).[30] Therefore, the MSPE method using the synthesized MIH-MIP could be practically applied for determining GLYP, AMPA, and GLUP in real samples. The enrichment factors calculated from the concentration ratios obtained by MSPE and direct HPLC were found to be 18, 14, and 9 for GLYP, AMPA, and GLUP, respectively. The precision values of the proposed methods, evaluated from the relative standard deviations (RSDs) of the peak areas from intraday (n = 7) and interday (n = 3 × 5) experiments, were better than 7 and 9%, respectively. The validation data of the developed MSPE-HPLC are summarized in Table 1.

2.6. Application to Real Samples. To demonstrate the applicability of the proposed MSPE-HPLC method in real samples, different types of water, soil, and vegetable samples were analyzed under optimized conditions. Matrix-matched calibration curves were prepared to evaluate any possible matrix effect. Matrix-matched standard solutions were prepared by adding the standard mixture to the blank sample. The matrix effect was estimated by the slope ratio of the calibration curves in the matrix and ultrapure water. The matrix effect values were found in the ranges of 0.20−1.69, 0.22−0.88, and 0.13−0.62 for water, soil, and vegetables, respectively. For this reason, the matrix-matched calibration method was used to diminish the sample matrix effects. The results demonstrated that GLYP and AMPA residues were detected at 0.85 and 0.87 mg kg^{-1}, respectively, in the studied Chinese cabbage samples, which were higher than the MRLs. The accuracy of the method was verified with recovery experiments by analyzing the samples spiked with standards at two concentration levels, at approximately LOQ (R_1) and approximately 5 times higher than LOQ concentrations (R_2). The recoveries of all analytes ranged from 86 to 118% with RSDs less than 10% (Table 2), meeting the requirements of pesticide residue analysis by the European Commission.[31] The acceptable recoveries with low RSDs demonstrated the successful applicability of the developed MSPE-HPLC method for the determination of GLYP, AMPA, and GLUP in various environmental samples.

https://doi.org/10.1021/acsomega.1c03488
ACS Omega 2021, 6, 27007−27016

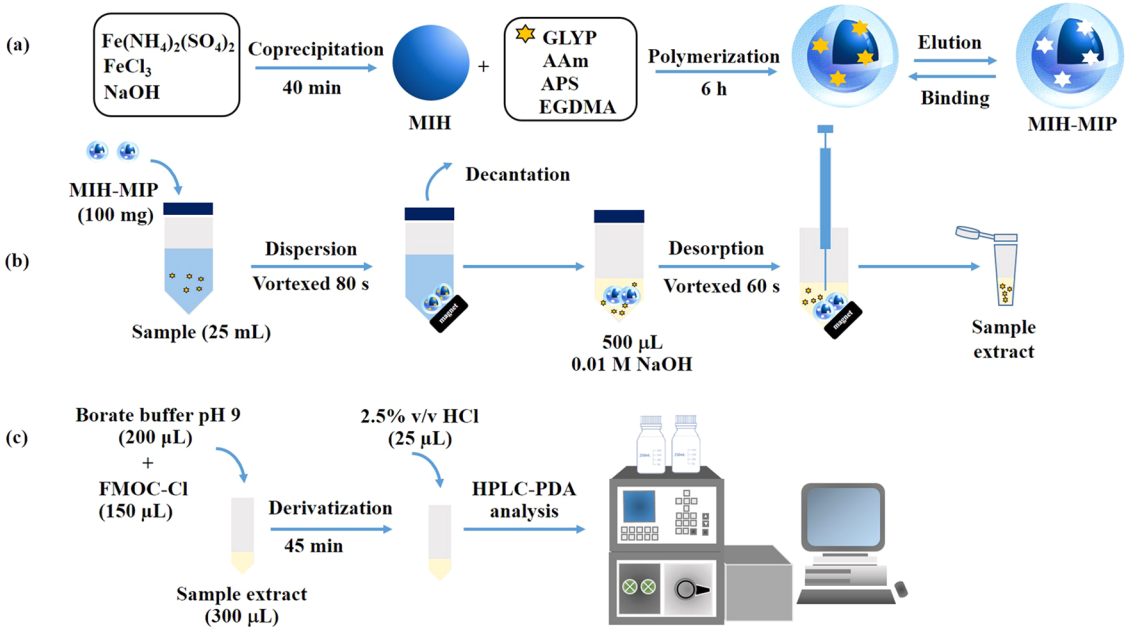

Figure 6. Schematic diagrams of (a) MIH-MIP synthesis, (b) MSPE procedure, and (c) precolumn derivatization HPLC analysis.

2.7. Comparison of the Proposed MSPE to Other Methods. The performance of the proposed MSPE method using novel MIH-MIP as a sorbent was compared with other previously reported sorbent-based extraction methods based on different MIPs for the determination of GLYP and other related compounds, as summarized in Table S3. The proposed method is reliable for GLYP analogues and provides wide linear calibration ranges as well as acceptable recoveries for determination in various environmental matrices. Considering the sensitivity, the obtained LODs and LOQs are lower than those of regulated MRLs and sufficient for real-world application. The method using a commercially available AFFINIMIP SPE Glyphosate-AMPA cartridge gave higher sensitivity in a water matrix. However, the proposed MSPE procedure showed a significant feature of a simple extraction process in a shorter extraction time (time consumption in both adsorption and desorption processes). The proposed MIH-MIP sorbent has a high adsorption capacity for the target analytes and could be rapidly separated from the solution using an external magnet. In addition, this is the first report of MMIP for the enrichment of GLYP analogue compounds.

3. CONCLUSIONS

In this work, a novel magnetic molecularly imprinted polymer was successfully synthesized from GLYP as a template and applied as an efficient sorbent for selective extraction of GLYP and its analogue compounds. Data obtained from adsorption experiments demonstrated the specific recognition site and binding characteristics of the synthesized sorbent toward the target analytes. The developed MSPE coupled to HPLC indicated good analytical performance for accurate determination of GLYP, AMPA, and GLUP in various environmental samples. This procedure possesses the advantages of simplicity, rapidness, high selectivity, and sensitivity, which meet the method requirements for EU standards; therefore, the developed procedure has the potential to be practically used for the determination of glyphosate residues in real samples.

4. EXPERIMENTAL SECTION

4.1. Chemicals and Reagents. All standards, including GLYP, AMPA, GLUP, glycine (GLYC), sarcosine (SAR), and monocrotophos (MONO), were used with a purity of ≥99%. GLYP, AMPA, and GLUP were obtained from Dr. Ehrenstorfer GmbH (Germany). GLYC was supplied by Sigma-Aldrich (Switzerland). MONO was supplied by Chem-Service (United States). SAR was purchased from Sigma-Aldrich (China). Stock standard solutions at a concentration of 1000 μg mL^{-1} were prepared in water. Working solutions were prepared daily by dilution with water. Deionized water (18.2 MΩ cm) used in all experiments was prepared by a RiOs Type I Simplicity 185 water purification system (Millipore).

Acetonitrile (isocratic grade, Merck, Germany), methanol (gradient grade, Merck, Germany), acetone (AR grade, Honeywell Riedel-de Haën, France), ammonia solution (AR grade, QRëC, New Zealand), and formic acid (AR grade, Merck, Germany) were used for extraction and HPLC separation. Iron(III) chloride anhydrous ($FeCl_3$, analysis grade, Riedel-de Haën, Germany), ammonium iron(II) sulfate hexahydrate ($Fe(NH_4)_2(SO_4)_2{\cdot}6H_2O$, AR grade, QRëC, New Zealand), and sodium hydroxide (NaOH, analysis grade, Merck, Germany) were utilized for the synthesis of MIH nanoparticles.

Acrylamide (AAm, AR grade, Sigma-Aldrich, China), ethylene glycol dimethacrylate (EGDMA, AR grade, Aldrich, China), and ammonium peroxodisulfate (APS, AR grade, AnalaR NORMAPUR, European community) were used for the synthesis of polymers. FMOC-Cl (AR grade, Aldrich, China) was used for derivatization. A 1500 mg L^{-1} FMOC-Cl solution was freshly prepared using acetonitrile as the solvent. Sodium tetraborate ($Na_2B_4O_7{\cdot}10H_2O$) and boric acid (H_3BO_3) were obtained from Kemaus (Australia) and used for the preparation of borate buffer (pH 9). Hydrochloric acid (AR grade, QRëC, New Zealand) was used in the derivatization procedure.

4.2. Instrumentation. Fourier transform infrared spectra were obtained on a PerkinElmer Spectrum One FTIR

https://doi.org/10.1021/acsomega.1c03488
ACS Omega 2021, 6, 27007−27016

spectrometer between 400 and 4000 cm^{-1} using a standard KBr disk method. A PANalytical EMPYREAN X-ray diffractometer (XRD) using monochromatic Cu Kα radiation (λ = 0.15406 nm) in a 2θ range of 10−80° was used for crystal structure characterization. The morphology and structure of the sorbent were analyzed using an FEI Helios NanoLab G3 CX dual-beam scanning electron microscope with a focused ion beam (FIB-SEM) and an FEI Tecnai G^2 20 transmission electron microscope working at a voltage of 200 kV. CHN analyses were performed using a PerkinElmer PE 2400 CHNS analyzer. The magnetic properties were measured using a Lake Shore (VSM 7403) vibrating sample magnetometer (VSM) at 298 K with an applied magnetic field (H) of ±10 000 Oersted (Oe).

The HPLC system consisted of an in-line degasser, a 600E quaternary pump, a Rheodyne injector with a 10 μL sample loop, a Waters 2996 photodiode array (PDA) detector, and Empower software for data acquisition (Waters). A Phenomenex Luna C18 (4.6 mm × 150 mm, 5 μm) column (Phenomenex) was used for the separation of the analyte derivatives. Separation was performed using acetonitrile (solvent A) and 0.1% formic acid (solvent B) as the mobile phase with a flow rate of 1.0 mL min^{-1}. The gradient elution was started at 35% solvent A for 3 min and ramped to 40% solvent A within 1 min. Then, solvent A was kept at 40% for 11 min followed by decreasing to 35% before starting the next run. Detection was performed at 265 nm for all analytes.

4.3. Synthesis of the Sorbents. MIH nanoparticles were prepared by coprecipitation of $Fe(NH_4)_2(SO_4)_2{\cdot}6H_2O$ and $FeCl_3$ (Figure 6a). Briefly, 7.922 g (0.020 mol) of $Fe(NH_4)_2(SO_4)_2{\cdot}6H_2O$ and 1.630 g (0.010 mol) of $FeCl_3$ were dissolved in 400 mL of deionized water and then stirred at room temperature for 20 min. Next, 50 mL of a 3 mol L^{-1} NaOH solution was quickly added. The resulting slurry was stirred for 20 min. The product was separated by an external magnet and rinsed with deionized water several times until obtaining pH ∼ 7. The obtained solid phase was washed with methanol and dried at 60 °C for 12 h.

The MIH-MIP sorbent was prepared by a polymerization procedure.[32] First, 5 mL of a 1 mg mL^{-1} GLYP solution was mixed with 0.568 g of AAm and 1 g of MIH in 200 mL of deionized water. Next, 4.5 mL of the cross-linker (EGDMA) was added, and the mixture was stirred at room temperature for 60 min. Then, 10 mL of the fresh radical initiator solution (8% w/v APS) was quickly added. The mixture was purged with nitrogen gas for 10 min and continuously stirred for 5 h to complete the polymerization process. The product was separated by an external magnet and dried at 60 °C for 12 h. The obtained material was stirred in a 0.01 mol L^{-1} NaOH solution for 3 h to remove the template. Finally, the MIH-MIP was rinsed several times with deionized water until obtaining pH ∼ 7. The sorbent was dried in a vacuum oven at 60 °C for 12 h. The mixed iron hydroxide-nonimprinted polymer (MIH-NIP) was prepared in the same manner without the addition of GLYP.

4.4. MSPE Procedure. In the present work, MIH-MIP was used as a sorbent material for the development of MSPE of GLYP, AMPA, and GLUP. A schematic diagram of the proposed MSPE procedure is presented in Figure 6b. First, 100 mg of the MIH-MIP sorbent was dispersed in 25 mL of the sample solution via vortex mixing for 80 s. Next, the analyte-extracted MIH-MIP sorbent was collected using an external magnet before decanting the supernatant. Then, a 0.01 mol L^{-1} NaOH solution (500 μL) was added, and the mixture was placed in a vortex mixer for 60 s to desorb the analytes from the sorbent. After separation of the MIH-MIP sorbent, the eluate was transferred to form a derivative with the FMOC-Cl reagent before further analysis by HPLC.

4.5. Derivatization Procedure. The precolumn derivatization of the target analytes was performed using the FMOC-Cl reagent.[33,34] First, 300 μL of the sample extract was mixed with 200 μL of 0.15 mol L^{-1} borate buffer pH 9 in a 15 mL centrifuge tube. After that, 150 μL of a 1500 mg L^{-1} FMOC-Cl solution was added. The mixture was vortexed for 30 s and kept at room temperature for 45 min. After that, 25 μL of 2.5% v/v HCl was added, and the solution was vortexed for 30 s to stop the reaction. Finally, the solution was filtered through a 0.45 μm nylon syringe filter and then injected into HPLC for analysis (Figure 6c).

4.6. Adsorption Experiments. *4.6.1. Static Adsorption.* To investigate the adsorption capacity of MIH-MIP and MIH-NIP sorbents, 25 mg of sorbent was added into 50 mL centrifuge tubes. Then, 10 mL of the mixed standard solution at concentrations varying from 2 to 60 mg L^{-1} was added. The mixture was vortexed for 80 s, and the sorbents were separated by an external magnet. The supernatant was collected and derivatized with FMOC-Cl before analysis by HPLC. The equilibrium adsorption capacity was calculated (eq 1).

$$Q_e = (C_0 - C_e) \times V/m \quad (1)$$

where Q_e is the amount of the analyte adsorbed by MIH-MIP or MIH-NIP (mg g^{-1}); C_0 and C_e are the initial and equilibrium concentrations of the standard solution (mg L^{-1}), respectively; V is the volume of the solution (mL); and m is the mass of the adsorbent (g).[27]

Scatchard's plot equation (eq 2) was used for further evaluation of the binding property of MIH-MIP or MIH-NIP.

$$Q_e/C_e = (Q_{max} - Q_e)/K_d \quad (2)$$

where Q_e is the adsorption capacity at adsorption equilibrium, C_e is the equilibrium concentration, Q_{max} is the apparent maximum adsorption capacity, and K_d is the dissociation constant.[35]

4.6.2. Dynamic Adsorption. Dynamic adsorption experiments were carried out to determine the adsorption mechanisms of the synthesized sorbents. MIH-MIP or MIH-NIP (25 mg) was added to 10 mL of a 20 mg L^{-1} standard solution in 50 mL centrifuge tubes. Then, the mixture was vortexed for 20, 40, 60, 80, and 100 s. The sorbents were magnetically separated. The supernatant was collected and derivatized with FMOC-Cl and analyzed by HPLC. The experimental data were evaluated by adsorption kinetic models (eqs 3 and 4).

$$\text{pseudofirst} - \text{order: } \ln(Q_e - Q_t) = \ln Q_{1cal} - k_1 t \quad (3)$$

$$\text{pseudosecond} - \text{order: } t/Q_t = 1/k_2 Q_{2cal}^2 + t/Q_{2cal} \quad (4)$$

where Q_e is the equilibrium adsorption capacity (mg g^{-1}); Q_{cal} is the theoretical adsorption capacity; Q_t is the adsorption capacity at time t; and k_1 and k_2 are the first-order and second-order rate constants, respectively.[27]

4.7. Selectivity Evaluation. To determine the selectivity of the synthesized MIH-MIP sorbent, similar structural compounds, including AMPA, GLUP, GLYC, SAR, and MONO, were tested as interfering molecules. MIH-MIP or

https://doi.org/10.1021/acsomega.1c03488
ACS Omega 2021, 6, 27007−27016

MIH-NIP sorbents (20 mg) were added to 10 mL of mixed solutions containing GLYP, AMPA, GLUP, GLY, SAR, and MONO at a concentration of 20 μg mL^{-1} each. The mixture was vortexed for 80 s. Then, the free target analytes and interfering molecules in the supernatant were derivatized with FMOC-Cl and analyzed using HPLC. The imprinting factor (IF) and selectivity coefficient (SC) were calculated (eqs 5 and 6).

$$IF = Q_{MIH-MIP}/Q_{MIH-MNIP} \quad (5)$$

$$SC = IF_t/IF_c \quad (6)$$

where $Q_{MIH-MIP}$ and $Q_{MIH-NIP}$ represent the adsorption capacities of MIH-MIP and MIH-NIP, respectively. IF_t is the imprinting factor for template molecules, and IF_c is the imprinting factor for structural or nonstructural analogues.[27]

4.8. Collection and Pretreatment of the Samples. Water, soil, and vegetable samples were collected from different sites in the northeastern area of Thailand. Agricultural water was collected from Maha Sarakham Province. Tap water, rice field water, and river water were collected from Khon Kaen Province. All samples were filtered through 0.45 μm nylon membrane filters and kept below 4 °C until analysis.

Two soil samples, including rice fields and agricultural soils, were collected from Khon Kaen Province. Soil samples were air-dried at room temperature, crushed, and then sieved to a particle size of 180 μm. The pretreatment method modified from a previous report was adopted.[36] Briefly, 2.5 g of homogenized soil was weighed into a 50 mL polypropylene centrifuge tube, and then 12.5 mL of a 0.6 mol L^{-1} KOH solution was added followed by vortexing for 2 min. After that, 12.5 mL of 0.6 mol L^{-1} HCl was added, and the pH was adjusted to 7 using 1 mol L^{-1} HCl. Thereafter, the supernatant was collected and filtered through a 0.45 μm nylon membrane filter before applying the MSPE procedure.

Chinese cabbage taken from a local market in Maha Sarakham Province and cabbage collected from a local market in Khon Kaen Province were analyzed. The samples were homogeneously blended and treated using the modified QuPPe method.[37] Briefly, the samples (2.5 g) were mixed with 12.5 mL of 0.1% formic acid in 50 mL polypropylene centrifuge tubes. Then, 12.5 mL of a 0.1% KOH solution was added, and the pH was adjusted to 7 using 1 mol L^{-1} KOH. The supernatant was collected and filtered through a 0.45 μm nylon membrane filter before analysis.

■ ASSOCIATED CONTENT

Supporting Information

The Supporting Information is available free of charge at https://pubs.acs.org/doi/10.1021/acsomega.1c03488.

FTIR spectra; XRD patterns; adsorption isotherms; fitting curves of Langmuir and Freundlich models; kinetic adsorption curves, pseudofirst-order and pseudo-second-order plots; effect of sample volume, sorbent amount, adsorption and desorption time, type of desorption and volume, and sample pH on the extraction efficiency of the MSPE procedure; Scatchard analysis of MIH-MIP and MIH-NIP; kinetic parameters for the binding of GLYP, AMPA, and GLUP to MIH-MIP and MIH-NIP; and comparison of the proposed MSPE method with other extraction methods based on MIP (PDF)

■ AUTHOR INFORMATION

Corresponding Author

Rodjana Burakham − *Materials Chemistry Research Center, Department of Chemistry, Faculty of Science, Khon Kaen University, Khon Kaen 40002, Thailand;* orcid.org/0000-0002-4786-9809; Phone: +66 4300 9700; Email: rodjbu@kku.ac.th; Fax: +66 4320 2373

Author

Nilawan Surapong − *Materials Chemistry Research Center, Department of Chemistry, Faculty of Science, Khon Kaen University, Khon Kaen 40002, Thailand*

Complete contact information is available at: https://pubs.acs.org/10.1021/acsomega.1c03488

Notes

The authors declare no competing financial interest.

■ ACKNOWLEDGMENTS

The authors gratefully acknowledge financial support from the Science Achievement Scholarship of Thailand. R.B. thanks the National Research Council of Thailand (NRCT) and Khon Kaen University for supporting the Mid-Career Research Grant (NRCT5-RSA63003-05). The authors also acknowledge support from the Materials Chemistry Research Center, Khon Kaen University, the Center of Excellence for Innovation in Chemistry (PERCH-CIC), and the Ministry of Higher Education, Science, Research, and Innovation (Implementation Unit-IU, Khon Kaen University).

■ REFERENCES

(1) Steinborn, A.; Alder, L.; Michalski, B.; Zomer, P.; Bendig, P.; Martinez, S. A.; Mol, H. G. J.; Class, T. J.; Pinheiro, N. C. Determination of glyphosate levels in breast milk samples from Germany by LC−MS/MS and GC−MS/MS. *J. Agric. Food Chem.* **2016**, *64*, 1414−1421.

(2) Koskinen, W. C.; Marek, L. J.; Hall, K. E. Analysis of glyphosate and aminomethylphosphonic acid in water, plant materials and soil. *Pest Manage. Sci.* **2016**, *72*, 423−432.

(3) Rigobello-Masini, M.; Pereira, E. A. O.; Abate, G.; Masini, J. C. Solid-phase extraction of glyphosate in the analyses of environmental, plant, and food samples. *Chromatographia* **2019**, *82*, 1121−1138.

(4) Mahmoudpour, M.; Torbati, M.; Mousavi, M. M.; de la Guardia, M.; Dolatabadi, J. E. N. Nanomaterial-based molecularly imprinted polymers for pesticides detection: Recent trends and future prospects. *TrAC, Trends Anal. Chem.* **2020**, *129*, No. 115943.

(5) Do, M. H.; Florea, A.; Farre, C.; Bonhomme, A.; Bessueille, F.; Vocanson, F.; Tran-Thi, N. T.; Jaffrezic-Renault, N. Molecularly imprinted polymer-based electrochemical sensor for the sensitive detection of glyphosate herbicide. *Int. J. Environ. Anal. Chem.* **2015**, *95*, 1489−1501.

(6) Zhang, C.; She, Y.; Li, T.; Zhao, F.; Jin, M.; Guo, Y.; Zheng, L.; Wang, S.; Jin, F.; Shao, H.; Liu, H.; Wang, J. A highly selective electrochemical sensor based on molecularly imprinted polypyrrole-modified gold electrode for the determination of glyphosate in cucumber and tap water. *Anal. Bioanal. Chem.* **2017**, *409*, 7133−7144.

(7) Zouaoui, F.; Bourouina-Bacha, S.; Bourouina, M.; Alcacer, A.; Bausells, J.; Jaffrezic-Renault, N.; Zine, N.; Errachid, A. Experimental study and mathematical modeling of a glyphosate impedimetric microsensor based on molecularly imprinted chitosan film. *Chemosensors* **2020**, *8*, No. 104.

(8) Sellergren, B. Imprinted chiral stationary phases in high-performance liquid Chromatography. *J. Chromatogr. A* **2001**, *906*, 227−252.

(9) Xia, J.; Yi, L.; MinJie, G.; Ying, W.; HuaiFeng, M. Separation/enrichment of the low-content high molecular weight natural protein using protein-imprinted polymers with ARPCs. *Sci. China, Ser. B: Chem.* **2009**, *52*, 1388−1393.
(10) da Mata, K.; Corazza, M. Z.; de Oliveira, F. M.; de Toffoli, A. L.; Tarley, C. R. T.; Moreira, A. B. Synthesis and characterization of cross-linked molecularly imprinted polyacrylamide for the extraction/preconcentration of glyphosate and aminomethylphosphonic acid from water samples. *React. Funct. Polym.* **2014**, *83*, 76−83.
(11) Puzio, K.; Claude, B.; Amalric, L.; Berho, C.; Grellet, E.; Bayoudh, S.; Nehmé, R.; Morin, P. Molecularly imprinted polymer dedicated to the extraction of glyphosate in natural waters. *J. Chromatogr. A* **2014**, *1361*, 1−8.
(12) Gomez-Caballero, A.; Diaz-Diaz, G.; Bengoetxea, O.; Quintela, A.; Unceta, N.; Goicolea, M. A.; Barrio, R. J. Water compatible stir-bar devices imprinted with underivatised glyphosate for selective sample clean-up. *J. Chromatogr. A* **2016**, *1451*, 23−32.
(13) Claude, B.; Berho, C.; Bayoudh, S.; Amalric, L.; Coisy, E.; Nehmé, R.; Morin, P. Preliminary recovery study of a commercial molecularly imprinted polymer for the extraction of glyphosate and AMPA in different environmental waters using MS. *Environ. Sci. Pollut. Res.* **2017**, *24*, 12293−12300.
(14) Ansari, S. Application of magnetic molecularly imprinted polymer as a versatile and highly selective tool in food and environmental analysis: recent developments and trends. *TrAC, Trends Anal. Chem.* **2017**, *90*, 89−106.
(15) Ilktaç, R.; Gümüş, Z. P. Magnetite-molecularly imprinted polymer based highly sensitive chromatographic method for preconcentration and determination of pirimicarb. *Int. J. Environ. Anal. Chem.* **2020**, 1−13.
(16) Zhao, Y.; Du, D.; Li, Q.; Chen, W.; Li, Q.; Zhang, Q.; Liang, N. Dummy-surface molecularly imprinted polymers based on magnetic graphene oxide for selective extraction and quantification of pyrethroids pesticides in fruit juices. *Microchem. J.* **2020**, *159*, No. 105411.
(17) Hu, X.; Chen, Y.; Xie, Z.; Zhang, L. Effective preparation of magnetic molecularly imprinted polymer nanoparticle for the rapid and selective extraction of Cyfluthrin from honeysuckle. *J. Biomater. Sci., Polym. Ed.* **2020**, *31*, 954−968.
(18) Zhao, F.; He, Y.; Zhang, C.; Ei-Aty, A. M. A.; Baranenko, D. A.; Hacimüftüoğlu, A.; She, Y. Assessment of magnetic core-shell mesoporous molecularly imprinted polymers for selective recognition of triazoles residual levels in cucumber. *J. Chromatogr. B* **2019**, *1132*, No. 121811.
(19) Ma, G.; Chen, L. Determination of chlorpyrifos in rice based on magnetic molecularly imprinted polymers coupled with high-performance liquid chromatography. *Food Anal. Methods* **2014**, *7*, 377−388.
(20) Liu, L.; Yang, M.; He, M.; Liu, T.; Chen, F.; Li, Y.; Feng, X.; Zhang, Y.; Zhang, F. Magnetic solid phase extraction sorbents using methyl-parathion and quinalphos dual-template imprinted polymers coupled with GC-MS for class-selective extraction of twelve organophosphorus pesticides. *Microchim. Acta* **2020**, *187*, No. 503.
(21) Mehdipour, M.; Ansari, M.; Pournamdari, M.; Zeidabadinejad, L.; Kazemipour, M. Selective extraction of malathion from biological fluids by molecularly imprinted polymer coated on spinel ZnFe2O4 magnetic nanoparticles based on green synthesis. *Sep. Sci. Technol.* **2021**, *56*, 1899−1909.
(22) Kumar, N.; Narayanan, N.; Gupta, S. Application of magnetic molecularly imprinted polymers for extraction of imidacloprid from eggplant and honey. *Food Chem.* **2018**, *255*, 81−88.
(23) Duan, G. W.; Zhang, J.; Li, Y.; Xu, Y. M.; Yin, F.; Fu, Y. Z. The preparation of Fe3O4/molecular-imprinted nanocomposite and the application on the recognition and separation of glyphosate. *Inorg. Nano-Met. Chem.* **2017**, *47*, 481−487.
(24) Obaidat, I. M.; Nayek, C.; Manna, K.; Bhattacharjee, G.; Al-Omari, I. A.; Gismelseed, A. Investigating exchange bias and coercivity in Fe3O4-γ-Fe2O3 core-shell nanoparticles of fixed core diameter and variable shell thicknesses. *Nanomaterials* **2017**, *7*, No. 415.
(25) Zhao, P.; Yan, M.; Zhang, C.; Peng, R.; Ma, D.; Yu, J. Determination of glyphosate in foodstuff by one novel chemiluminescence-molecular imprinting sensor. *Spectrochim. Acta, Part A* **2011**, *78*, 1482−1486.
(26) Wang, L.; Shi, C.; Wang, L.; Pan, L.; Zhang, X.; Zou, J. J. Rational design, synthesis, adsorption principles and applications of metal oxide adsorbents: A review. *Nanoscale* **2020**, *12*, 4790−4815.
(27) Chen, S.; Fu, J.; Li, Z.; Zeng, Y.; Li, Y.; Su, X.; Jiang, X.; Yang, H.; Huang, L.; Zou, L.; He, L.; Liu, S.; Ao, X.; Yang, Y. Preparation and application of magnetic molecular imprinted polymers for extraction of cephalexin from pork and milk samples. *J. Chromatogr. A* **2019**, *1602*, 124−134.
(28) Bui, B. T. S.; Haupt, K. Molecularly imprinted polymers: synthetic receptors in bioanalysis. *Anal. Bioanal. Chem.* **2010**, *398*, 2481−2492.
(29) Piriyapittaya, M.; Jayanta, S.; Mitra, S.; Leepipatpiboon, N. Micro-scale membrane extraction of glyphosate and aminomethylphosphonic acid in water followed by high-performance liquid chromatography and post-column derivatization with fluorescence detector. *J. Chromatogr. A* **2008**, *1189*, 483−492.
(30) European Commission. 2005. REGULATION (EC) NO 396/2005 OF THE EUROPEAN PARLIAMENT AND OF THE COUNCIL of 23 February 2005 on maximum residue levels of pesticides in or on food and feed of plant and animal origin and amending Council Directive 91/414/EEC. *Off. J. Eur. Union* **2005**, *50*, 1−50.
(31) European Commission. *Analytical Quality Control and Method Validation Procedures for Pesticides Residues Analysis in Food and Feed*; Document No. SANTE/12682/2019; EURL, 2020.
(32) Harsini, N. N.; Ansari, M.; Kazemipour, M. Synthesis of molecularly imprinted polymer on magnetic core-shell silica nanoparticles for recognition of congo red. *Eurasian J. Anal. Chem.* **2018**, *13*, No. em20.
(33) Gomez-Caballero, A.; Diaz-Diaz, G.; Bengoetxea, O.; Quintela, A.; Unceta, N.; Goicolea, M. A.; Barrio, R. J. Water compatible stir-bar devices imprinted with underivatized glyphosate for selective sample clean-up. *J. Chromatogr. A* **2016**, *1451*, 23−32.
(34) Schrübbers, L. C.; Masís-Mora, M.; Rojas, E. C.; Valverde, B. E.; Christensen, J. H.; Cedergreen, N. Analysis of glyphosate and aminomethylphosphonic acid in leaves from Coffea arabica using high performance liquid chromatography with quadrupole mass spectrometry detection. *Talanta* **2016**, *146*, 609−620.
(35) Huang, Y.; Pan, J.; Liu, Y.; Wang, M.; Deng, S.; Xia, Z. A SPE method with two MIPs in two steps for improving the selectivity of MIPs. *Anal. Chem.* **2019**, *91*, 8436−8442.
(36) Ibáñez, M.; Pozo, ÓJ.; Sancho, J. V.; López, F. J.; Hernández, F. Residue determination of glyphosate, glufosinate and aminomethylphosphonic acid in water and soil samples by liquid chromatography coupled to electrospray tandem mass spectrometry. *J. Chromatogr. A* **2005**, *1081*, 145−155.
(37) Anastassiades, M.; Kolberg, D. I.; Eichhorn, E.; Benkenstein, A.; Lukačević, S.; Mack, D.; Wildgrube, C.; Sigalov, I.; Dörk, D.; Barth, A. *Quick Method for the Analysis of Residues of Numerous Highly Polar Pesticides in Foods of Plant Origin via LC-MS/MS Involving Simultaneous Extraction with Methanol (QuPPe-Method)*; EURL-SRM: Stuttgart, Germany, 2015; Vol. *58*, pp 1−6.

https://doi.org/10.1021/acsomega.1c03488
ACS Omega 2021, 6, 27007−27016